

## CHAPTER IV - NUMERICAL TECHNIQUE AND PROGRAM FOR FINITE ELEMENT CONSTITUTIVE CRACKING ANALYSIS

The main purpose of this chapter is to develop a sub-program which is to be incorporated into the commercial general-purpose finite element (FE) program – MSC.Marc – and to test the sub-program using elementary, simple specimens of both plane stress and plane strain elements. The sub-program should have the capacity to simulate the cracking process in concrete, using the adopted constitutive relationships of crack softening outlined in Chapter III.

Very few general-purpose commercial FE packages can accommodate the non-linear cracking analysis of concrete structures. MSC.Marc is an FE program which can model concrete cracking with linear post-peak strain softening and a constant shear retention factor  $\beta$ . Bilinear or non-linear strain softening, and arbitrary crack-opening-dependent reduced shear modulus in the constitutive modelling of concrete cracking are not available in this program. However, MSC.Marc allows users to develop and substitute their own sub-programs in the package. This feature provides users with a powerful way of solving non-standard problems, such as crack simulation in concrete. The program was available for the author to use for this research.

The FE method basically has six steps. The success of any FE program depends partly on how the program implements these steps. A description of the FE method (including the following six steps) and the algorithm used in MSC.Marc is given in the Annexure.

**Step 1: Choose shape functions**

**Step 2: Establish material relationship**

**Step 3: Compile element matrices**

**Step 4: Assemble to form the overall structural stiffness matrix**

**Step 5: Solve equations**

**Step 6: Recover the stresses and strains.**

#### 4.1 Program framework for the cracking analysis of concrete

##### 4.1.1 Framework for the implementation of the constitutive model in the FE analysis of concrete structures

The flow chart shown in Figure 4.1 illustrates the general FE procedure for the crack analysis of concrete structures.

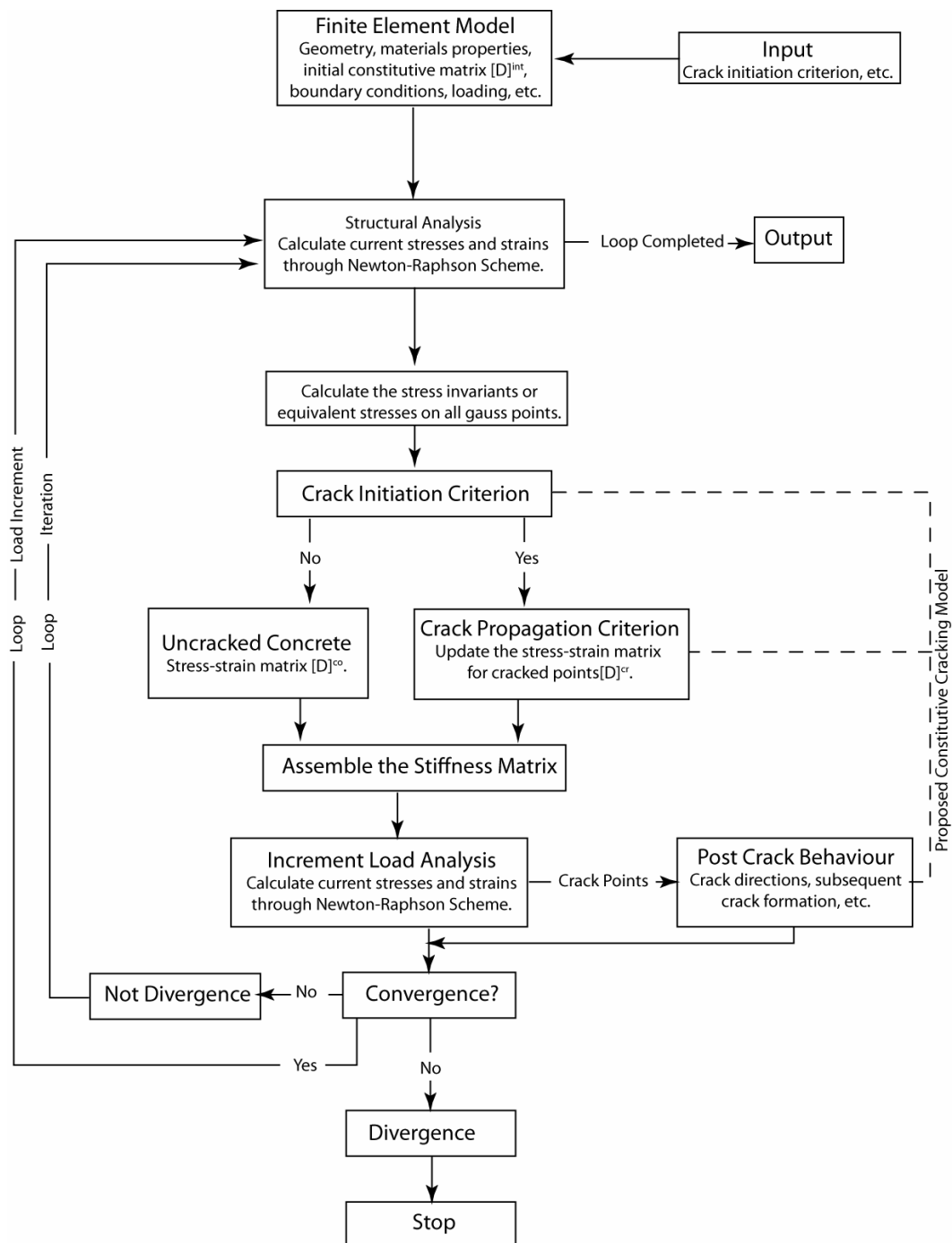


Figure 4.1 - General FE crack analysis procedure for concrete structures

#### 4.1.2 Sub-program coded in MSC.Marc to implement the crack constitutive model

Modelling bilinear or non-linear mode I and II softening requires the development and programming of a subroutine in MSC.Marc. The lack of advanced fracture-modelling capacity in this FE package (and in other generally available FE packages) requires a considerable programming effort to implement crack modelling.

A subprogram called HYPELA, incorporated into MSC.Marc, was specially and independently developed for this research on the FE modelling of the cracking behaviour of concrete structures. The subroutine has the capacity to simulate the cracking process in concrete, using the adopted constitutive relationships of crack softening outlined in Chapter III.

The cracking analysis starts with the linear elastic stress-strain law. In the subprogram HYPELA, the following steps are performed (refer to Figure 4.2 for the flowchart of these steps):

**Step 1:** Material properties and parameters related to concrete strain softening, such as the fracture energy  $G_f$ , Young's modulus  $E$ , Poisson's ratio  $\nu$ , tensile strength  $f_t$ , mode I softening parameters  $(\alpha_1 / \alpha_2)$ , maximum mode II shear reduced factor  $\beta_{max}$ , etc. are input for a specific crack analysis application.

**Step 2:** The utility routine ELMVAR is called to retrieve element data (e.g. stresses  $\sigma_{ij}$ , strains  $\varepsilon_{ij}$ ) from the MSC.Marc program's internal data storage. ELMVAR is provided with the following information: element post code (icode); element number (m); integration point number (nn); layer number (kc) and requested variables (var).

**Step 3:** A further subroutine – STRM – was specially coded for this research to be called in the subprogram HYPELA in order to calculate the principal stresses and their direction

cosines from the stress tensor  $\sigma_{ij} = \begin{bmatrix} \sigma_{11} & \sigma_{12} & \sigma_{13} \\ \sigma_{21} & \sigma_{22} & \sigma_{23} \\ \sigma_{31} & \sigma_{32} & \sigma_{33} \end{bmatrix}$  retrieved by ELMVAR at any Gauss

point.

In the subroutine STRM, the principal stresses and direction cosines at a Gauss point are calculated as follows (refer to Chen 1982):

- Calculate the first invariant of the stress tensor:  $I_1 = \sigma_{11} + \sigma_{22} + \sigma_{33}$  (4.1)

- Calculate the mean normal stress:  $\sigma_m = \frac{1}{3}I_1$  (4.2)

- Obtain the stress deviator tensor  $S_{ij} = \begin{bmatrix} \sigma_{11} - \sigma_m & \sigma_{12} & \sigma_{13} \\ \sigma_{21} & \sigma_{22} - \sigma_m & \sigma_{23} \\ \sigma_{31} & \sigma_{32} & \sigma_{33} - \sigma_m \end{bmatrix}$  (4.3)

- Calculate the second invariant of the stress tensor:

$$J_2 = \frac{1}{2}S_{ij}S_{ij} = \frac{1}{2}(S_{11}^2 + S_{22}^2 + S_{33}^2) + S_{12}^2 + S_{23}^2 + S_{31}^2 \quad (4.4)$$

- Calculate the third invariant of the stress tensor:

$$J_3 = \frac{1}{3}S_{ij}S_{jk}S_{ki} = S_{11}S_{22}S_{33} + 2S_{12}S_{23}S_{31} - S_{11}S_{23}^2 - S_{22}S_{13}^2 - S_{33}S_{12}^2 \quad (4.5)$$

- Calculate  $\cos 3\theta = \frac{3\sqrt{3}}{2} \frac{J_3}{\sqrt{J_2^3}}$  (4.6)

where  $\theta$  is the angle of similarity.

- Calculate the principal stresses:

$$\begin{bmatrix} \sigma_1 \\ \sigma_2 \\ \sigma_3 \end{bmatrix} = \begin{bmatrix} S_1 \\ S_2 \\ S_3 \end{bmatrix} + \sigma_m \begin{bmatrix} 1 \\ 1 \\ 1 \end{bmatrix} = \frac{2\sqrt{J_2}}{\sqrt{3}} \begin{bmatrix} \cos \theta \\ \cos(\theta - \frac{2}{3}\pi) \\ \cos(\theta + \frac{2}{3}\pi) \end{bmatrix} + \frac{I_1}{3} \begin{bmatrix} 1 \\ 1 \\ 1 \end{bmatrix} \quad (4.7)$$

- Set  $\sigma = \sigma_1$ , solve 
$$\begin{bmatrix} \sigma_{11} - \sigma_1 & \sigma_{12} & \sigma_{13} \\ \sigma_{21} & \sigma_{22} - \sigma_1 & \sigma_{23} \\ \sigma_{31} & \sigma_{32} & \sigma_{33} - \sigma_1 \end{bmatrix} \begin{bmatrix} l_1 \\ m_1 \\ n_1 \end{bmatrix} = \begin{bmatrix} 0 \\ 0 \\ 0 \end{bmatrix} \quad (4.8)$$

and  $l_1^2 + m_1^2 + n_1^2 = 1$ ; (4.9)

The Cramer method in matrix algebra is adopted to obtain the direction cosines of the first principal stress to the global coordinates  $l_1$ ,  $m_1$  and  $n_1$ .

- Similarly, set  $\sigma = \sigma_2$  and  $\sigma = \sigma_3$  to obtain the direction cosines of the second and third principal stresses to the global coordinates  $l_2$ ,  $m_2$ ,  $n_2$  and  $l_3$ ,  $m_3$ ,  $n_3$  respectively.

**Step 4:** Check the crack initiation criterion ( $\sigma_1 \geq f_t$ ) for a Gauss point which has not cracked before. Also check new crack conditions for an existing crack at a Gauss point ( $\sigma_1 \geq f_t$ , or whether the angle between the previous crack and the present crack at a Gauss point is greater than the threshold angle). For a Gauss point that has not cracked before, if the crack initiation criterion is met, then the point is assumed to be cracking. Otherwise, the point remains linear elastic. For an existing crack point, if either of the conditions is met, then a new additional crack is assumed at that point, at an angle to the previous crack.

**Step 5:** For the cracking points, using the direction cosines calculated from STRM, form the transformation matrix  $N = [N_1 \ N_2 \ \dots]$  (see equations 3.9, 3.26 and 3.30 in Chapter III for 3-D, plane stress and plane strain application respectively) and transform the strains from global coordinates to local coordinates.

**Step 6:** Check the status of stress and strain at the cracking points to see if the crack is still opening, or unloading/reloading, or closing (see Figures 3.9 and 3.10).

**Step 7:** According to the different crack statuses, define the mode I stiffness modulus  $D_i'$  for crack opening, or crack unloading/reloading, or crack closing accordingly in

$$D_i^{cr} = \begin{bmatrix} D_i^I & 0 & 0 \\ 0 & D_i^{II} & 0 \\ 0 & 0 & D_i^{III} \end{bmatrix} \text{ for the constitutive matrix } D^{cr} \text{ (refer to equation 3.16 and$$

Figures 3.9 and 3.10 in Chapter III). After that, form the constitutive relationship of equation 3.22.

**Step 8:** Transform the stresses and the stiffness matrix from local coordinates to global coordinates.

In the subprogram, the transformation of stresses, strains and the stiffness matrix between the global and local coordinate systems is carried out using the following equations (4.13 to 4.15):

Transformation matrix R, in which  $l_1, l_2, l_3, m_1, m_2, m_3, n_1, n_2, n_3$  are the direction cosines of the axes defined in Tables 3-1 and 3-2 in Chapter III, is as follows:

For 3-D analysis:

$$[R] = \begin{bmatrix} l_1^2 & m_1^2 & n_1^2 & l_1 m_1 & m_1 n_1 & n_1 l_1 \\ l_2^2 & m_2^2 & n_2^2 & l_2 m_2 & m_2 n_2 & n_2 l_2 \\ l_3^2 & m_3^2 & n_3^2 & l_3 m_3 & m_3 n_3 & n_3 l_3 \\ 2l_1 l_2 & 2m_1 m_2 & 2n_1 n_2 & l_1 m_2 + l_2 m_1 & m_1 n_2 + m_2 n_1 & n_1 l_2 + n_2 l_1 \\ 2l_2 l_3 & 2m_2 m_3 & 2n_2 n_3 & l_2 m_3 + l_3 m_2 & m_2 n_3 + m_3 n_2 & n_2 l_3 + n_3 l_2 \\ 2l_3 l_1 & 2m_3 m_1 & 2n_3 n_1 & l_3 m_1 + l_1 m_3 & m_3 n_1 + m_1 n_3 & n_3 l_1 + n_1 l_3 \end{bmatrix} \quad (4.10)$$

For 2-D plane stress analysis:

$$[R] = \begin{bmatrix} l_1^2 & m_1^2 & l_1 m_1 \\ l_2^2 & m_2^2 & l_2 m_2 \\ 2l_1 l_2 & 2m_1 m_2 & l_1 m_2 + l_2 m_1 \end{bmatrix} = \begin{bmatrix} \cos^2 \theta & \sin^2 \theta & \cos \theta \sin \theta \\ \sin^2 \theta & \cos^2 \theta & -\cos \theta \sin \theta \\ -2 \cos \theta \sin \theta & 2 \cos \theta \sin \theta & \cos^2 \theta - \sin^2 \theta \end{bmatrix} \quad (4.11)$$

For 2-D plane strain analysis:

$$[R] = \begin{bmatrix} l_1^2 & m_1^2 & n_1^2 & l_1 m_1 \\ l_2^2 & m_2^2 & n_2^2 & l_2 m_2 \\ l_3^2 & m_3^2 & n_3^2 & l_3 m_3 \\ 2l_1 l_2 & 2m_1 m_2 & 2n_1 n_2 & l_1 m_2 + l_2 m_1 \end{bmatrix} = \begin{bmatrix} \cos^2 \theta & \sin^2 \theta & 0 & \cos \theta \sin \theta \\ \sin^2 \theta & \cos^2 \theta & 0 & -\cos \theta \sin \theta \\ 0 & 0 & 1 & 0 \\ -2\cos \theta \sin \theta & 2\cos \theta \sin \theta & 0 & \cos^2 \theta - \sin^2 \theta \end{bmatrix} \quad (4.12)$$

$$\{\varepsilon'\} = [R]\{\varepsilon\}; \quad \{\varepsilon\} = [R]^{-1} \{\varepsilon'\} \quad (4.13)$$

$$\{\sigma'\} = [R]^{-T} \{\sigma\}; \quad \{\sigma\} = [R]^T \{\sigma'\} \quad (4.14)$$

$$[K'] = [R]^{-T} [K] [R]^{-1}; \quad [K] = [R]^T [K'] [R] \quad (4.15)$$

Where  $\{\varepsilon'\}$  is the local strain vector;  $\{\varepsilon\}$  is the global strain vector  
 $\{\sigma'\}$  is the local stress vector;  $\{\sigma\}$  is the global stress vector  
 $[K']$  is the local constitutive matrix;  $[K]$  is the global constitutive matrix.

**Step 9:** Return to the main program – MSC.Marc.

The HYPELA subprogram developed has the overall organization for the coding process as shown in Figure 4.2.

#### 4.1.3 Possible numerical implementation problems

In the implementation of the constitutive model, concrete fracture modelling problems could be encountered, such as snap-back, non-convergence or hour-glass modes.

‘Snap-back’ behaviour (in which the deflection response decreases after peak-point loading) could occur in the strain-softening analysis of concrete structures (Rots & de Borst 1987). Normal direct displacement control, installed in general FE programs, was demonstrated as being inadequate in modelling this “dramatic” behaviour to get a fully converged solution after peak load (de Borst 1986). An indirect displacement control technique, developed by de Borst (1986) for snap-back behaviour, has proved to be successful. However, this technique could not be implemented in MSC.Marc due to the

limitations of the package. In general, the limitations of FE packages require a special solution strategy to solve snap-back problems. The implementation of such a solution strategy is demonstrated in verification case 2 in Chapter V.

Non-convergence is a problem frequently encountered in highly non-linear analyses. The computation process is terminated at the stage where numerical difficulties, which can be caused by many factors (such as an ill-conditioned stiffness matrix or unstable crack propagation) cannot be overcome.

A further potential problem in modelling the cracking of concrete is ‘hour-glass’ modes, which have been reported by several researchers (de Borst 1986; Rots & de Borst 1987). These are spurious zero-energy modes that could cause non-convergence by developing a singular, or nearly singular, global stiffness matrix. They are often encountered when using reduced integration, although full-integration elements are not free from this phenomenon. Mixed-mode softening (normal and shear softening) and multiple crack simulation are potential factors that could trigger hour-glass modes.



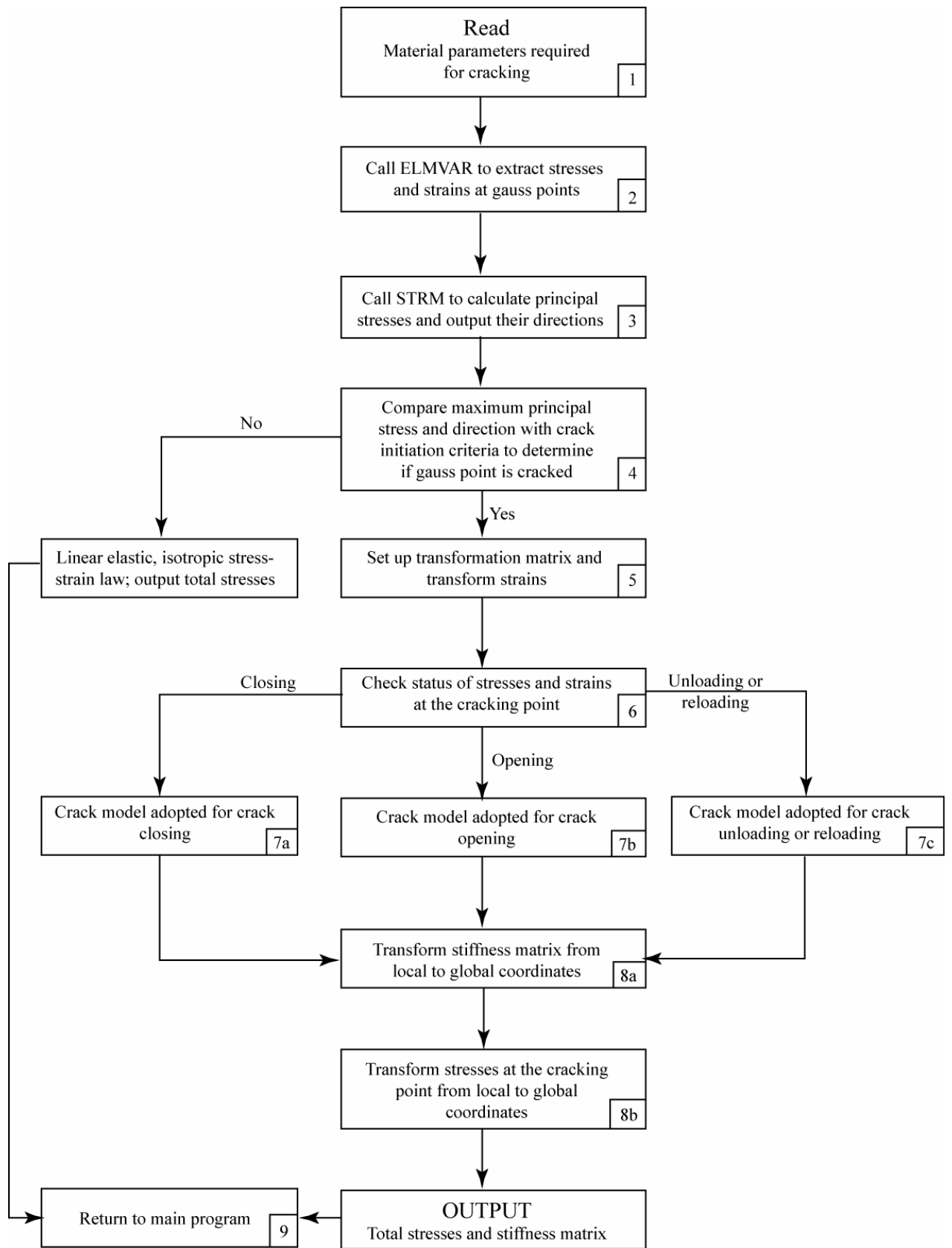


Figure 4.2 - Flow chart of the overall organization for coding the sub-program HYPELA

To save computer time, two groups of elements could be defined in the FE model: (1) elements that are not allowed to crack for the region where cracking under the given loadings is unlikely; and (2) elements which could possibly crack. The elements that could crack are called by the subprogram HYPELA, developed as explained above. The elements that are defined as not cracking are run as normal in MSC.Marc. The flow diagram in Figure 4.3 illustrates the implementation position of the subprogram HYPELA in the FE process of MSC.Marc.

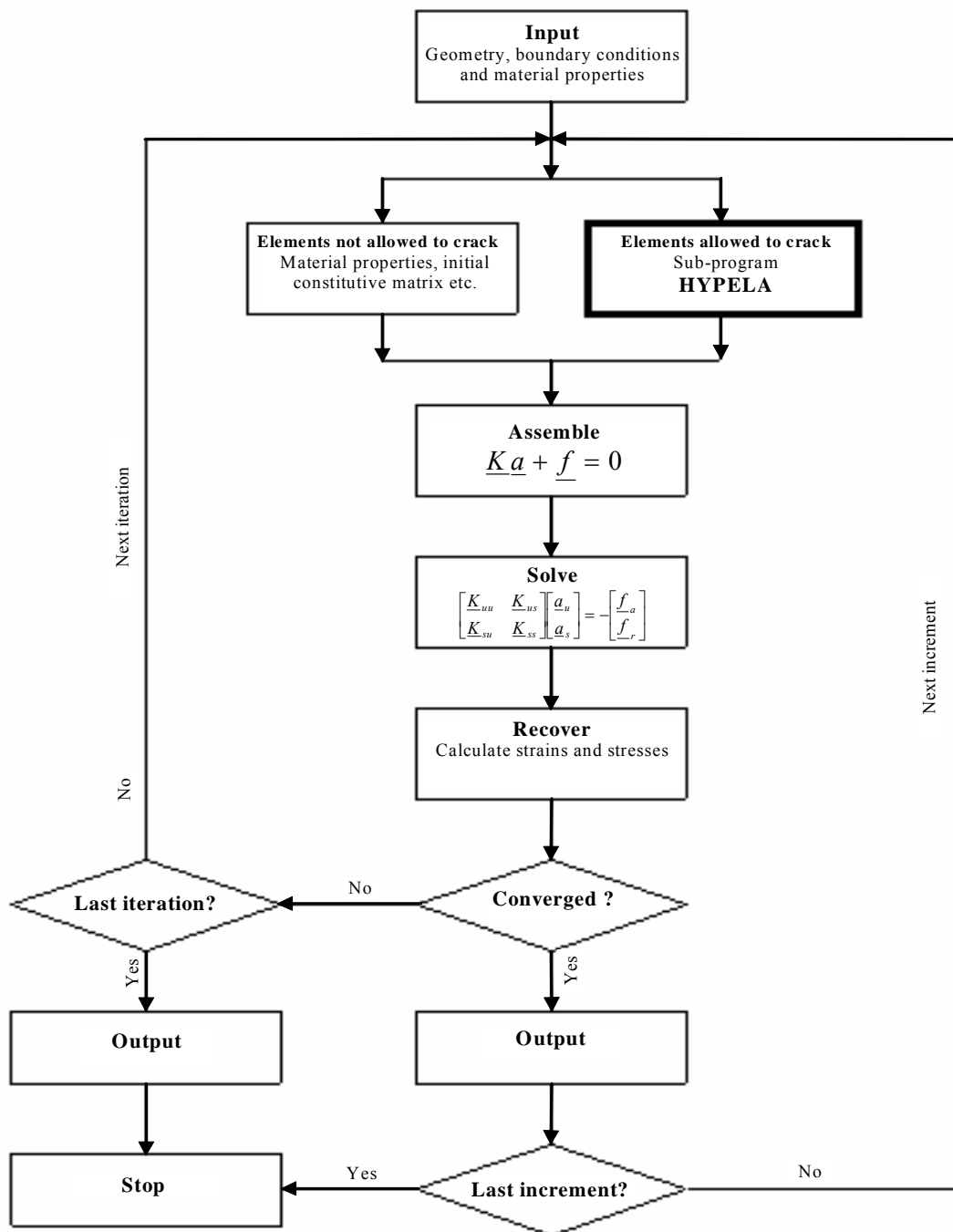


Figure 4.3 - Flow diagram for finite element analysis process in MSC.Marc

## 4.2 Verification study with MSC.Marc and other specimens investigated in the past

For the purpose of verifying the general application of the subroutine developed, it is logical to test the subroutine thoroughly on specimens that are fracture-sensitive.

Prior to cracking, concrete is assumed to be linear elastic and isotropic until the maximum principal stress exceeds the material's tensile strength. When this strength-based crack-initiating criterion is violated, cracks form in the direction perpendicular to the maximum principal stress. The strain-softening process starts at those Gauss points by moderating the isotropic, linear elastic stress-strain stiffness matrix to the adopted cracking stress-strain laws that have been selected for this testing purpose.

Four cases – called specimens 1, 2, 3 and 4 using plane stress elements, are verified in this section.

### 4.2.1 Built-in crack model in MSC.Marc for specimens 1 and 2 (with reference to MSC.Marc *Volume A: Theory and User Information*)

MSC.Marc has a built-in cracking model that can be used to handle concrete and other low-tension material. The model can predict crack initiation and simulate tension softening, plastic yielding and crushing. The cracking model is built on the uniaxial stress-strain diagram shown in Figure 4.4.

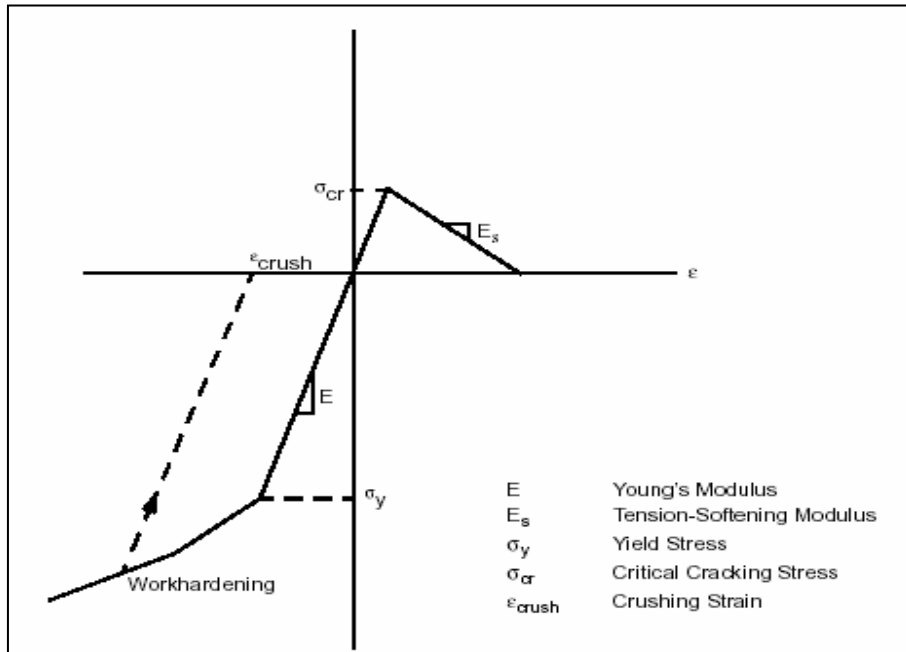


Figure 4.4 - Uniaxial stress-strain diagram

In this model, a crack develops in a material perpendicular to the direction of the maximum principal stress if the maximum principal stress  $\sigma_1$  in the material exceeds a certain value  $\sigma_{cr}$  (see Figure 4.4 and Figure 3.1 in Chapter III). Linear tension softening, characterized by a descending branch as shown Figure 4.4, is then adopted. The shear modulus across the crack is reduced by a constant shear retention factor. This model is by nature an orthotropic model, similar to the mode I and II improved Rashid model (smeared model 3 in Chapter II). At a material point, a second crack can only form perpendicular to the first crack.

An opened crack can close again if the loading is reversed. If crack closing occurs, it is assumed that the crack has the capability to carry full compressive stress.

#### 4.2.2 The smeared model adopted for specimens 1 and 2

In Chapter II, all the major crack models are reviewed and elaborated on. The crack model adopted for this verification purpose is briefly as follows:

**Verification crack model** (refer to smeared model 3 in Chapter II for a description of the mode). This model is used for verification purposes mainly for two reasons:

1. It is similar to the built-in crack model in MSC.Marc and can be used to validate the subprogram by comparing the results from the two methods.
2. It has the general capacity to model mode I and II fracturing in concrete.

#### 4.2.3 The smeared crack model adopted for specimens 3 and 4

The non-orthogonal, multi-directional crack models outlined in Chapter III that are implemented in the subprogram HYPELA are used to verify specimens 3 and 4 in this section.

#### 4.2.4 FE models benchmarked

Four test specimens are designed or selected for the verification exercise. Due to the fact that the built-in crack model in MSC.Marc can only handle linear mode I softening and a constant shear retention factor  $\beta$  to account for the loss of shear modulus after cracks, only the elementary simple-tension specimens (specimens 1 and 2) are believed to be adequate for the verification of the subprogram in the application of basic NLFM analysis. The results obtained from the subprogram are compared with the related results from either the built-in elastic, linear softening crack model in MSC.Marc or those from past investigations.

#### **Description of the element type and solution method used for the verification**

For this verification, a four-node quadrilateral isoparametric element with bilinear interpolation is adopted. A full 2 x 2 Gauss integration (four integration points) rule is used for the computation of the element stiffness matrix (see Figure 4.5). All the specimens used for verification purposes in this section are modelled as plane stress elements.

Each node in the element has two degrees of freedom ( $U_x$ ,  $U_y$ ), which results in a total of eight degrees of freedom in one single element.

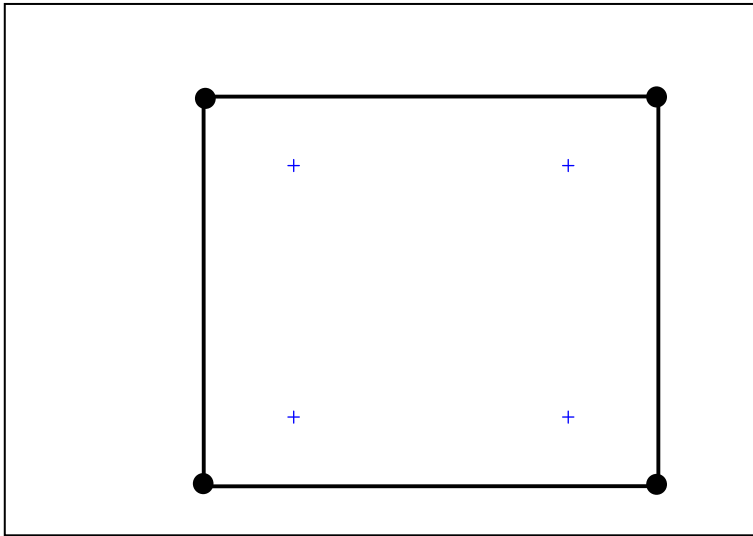


Figure 4.5 - First-order plane stress element with full integration

The element is formed by mapping from the  $x$ - $y$  plane to the  $\xi, \eta$  plane. Both the mapping and the assumed displacement function take the form:

$$x = a_0 + a_1 \xi + a_2 \eta + a_3 \xi \eta \quad (4.16)$$

$$y = b_0 + b_1 \xi + b_2 \eta + b_3 \xi \eta \quad (4.17)$$

Either the coordinate or the displacement function can be expressed in terms of the nodal quantities by the interpolation functions.

$$x = \sum_{i=1}^4 x_i \phi_i \quad (4.18)$$

Where

$$\phi_1 = \frac{1}{4}(1 - \xi)(1 - \eta)$$

$$\phi_2 = \frac{1}{4}(1 + \xi)(1 - \eta)$$

$$\phi_3 = \frac{1}{4}(1 + \xi)(1 + \eta)$$

$$\phi_4 = \frac{1}{4}(1 - \xi)(1 + \eta)$$

The full Newton-Raphson method is adopted for the solution of the stiffness formulation.

An adapted stepping procedure is adopted to automatically adjust the step time in the increment.

Convergence: the relative residual criterion is used with the default tolerance  $Tol = 0.01$  (see equation A.15)

### **Description of the test specimens used for the verification**

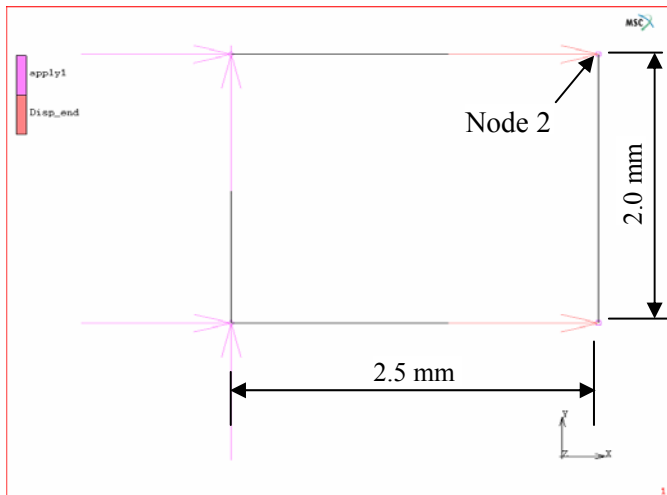
Un-reinforced concrete structures are the most fracture-sensitive. Plain concrete uniaxial tension specimens are probably more sensitive to fracture than any other type. For this reason, the following four plain concrete specimens are believed to provide a good test for the fracture sensitivity of the FE crack models.

**1). Specimen 1** (tension specimen with one side fixed and node displacements applied at the other end – Figure 4.6). This model is considered for the purpose of checking the accuracy of the stress-update procedure in the subprogram.

The crack directions are fixed after the cracks have formed. Three mode I linear softening moduli  $E_s$  of 2 000, 20 000 and 50 000 MPa are adopted to test the sensitivity of the subprogram to the mode I softening parameters. An arbitrary non-zero shear retention factor  $\beta$  is selected to stabilize the numerical solution as the  $\beta$  value will not influence the response of this pure tensile fracture mode I analysis. The built-in crack model in MSC.Marc is also run for the same crack parameters for this verification purpose.

The material properties and crack softening parameters are shown in Figure 4.6.

An increase in node displacements is applied gradually up to the maximum value and then gradually released to zero as shown in Figure 4.7.



Young's modulus  $E = 20\,000$  MPa  
 Poisson's ratio  $\nu = 0$   
 Tensile strength  $f_t = 1.2$  MPa  
 Shear retention factor  $\beta = 0.2$  (arbitrary)  
 Applied node displacement = 0.0008 mm

Figure 4.6 - FE model and model input (specimen 1)

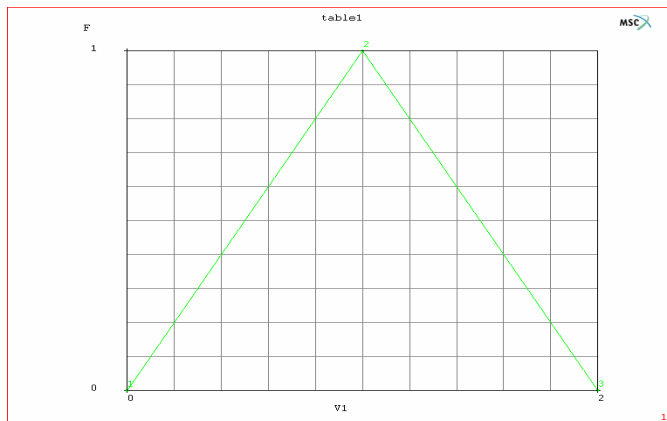


Figure 4.7 - Applied displacement load vs. time (specimen 1)

**2). Specimen 2** (tension specimen of four elements fixed at one end and node displacements applied at the other end – Figure 4.8). This model was designed to further test the subprogram developed for correct stress-strain interaction between the cracked element and neighbouring uncracked elements. Only one element adjacent to the fixed boundary is allowed to soften, as shown in Figure 4.9.

Similar to specimen 1, the crack directions are fixed after the cracks have formed. Three mode I linear softening moduli  $E_s$  of 2 000, 5 000 and 20 000 MPa are adopted to test the sensitivity and correctness of the program to the mode I softening parameters. Again, an arbitrary non-zero shear retention factor  $\beta$  is selected only to stabilize the numerical solution as the  $\beta$  value will not influence the response of this pure tensile fracture mode I



analysis. The built-in crack model in MSC.Marc is also run for the same crack parameters for this verification purpose.

The material properties and crack softening parameters are shown in Figure 4.8.

An increase in node displacements is applied gradually up to the maximum value and then gradually released to zero, as shown in Figure 4.10.

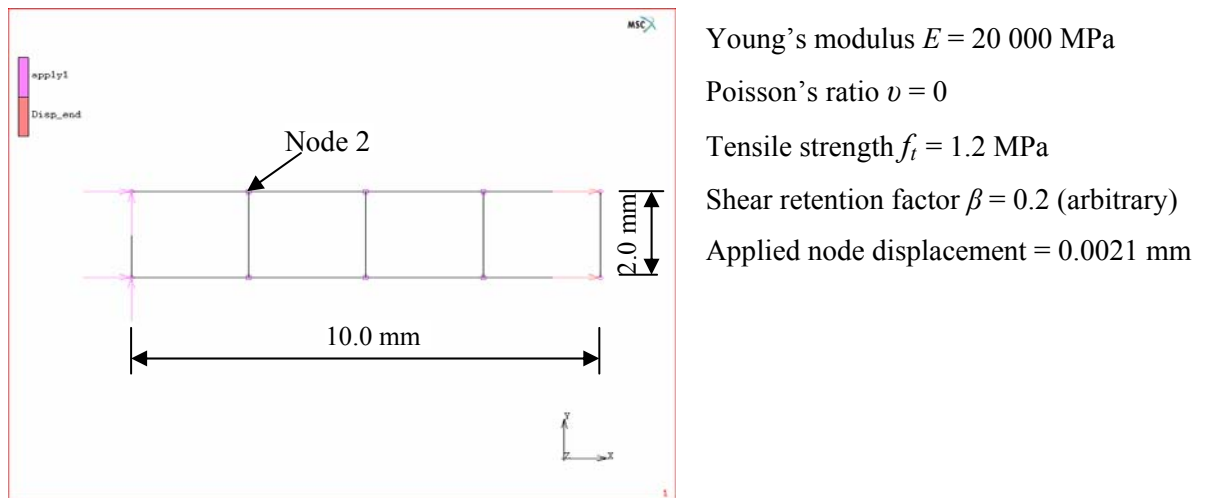


Figure 4.8 - FE model – beam of four elements (specimen 2)

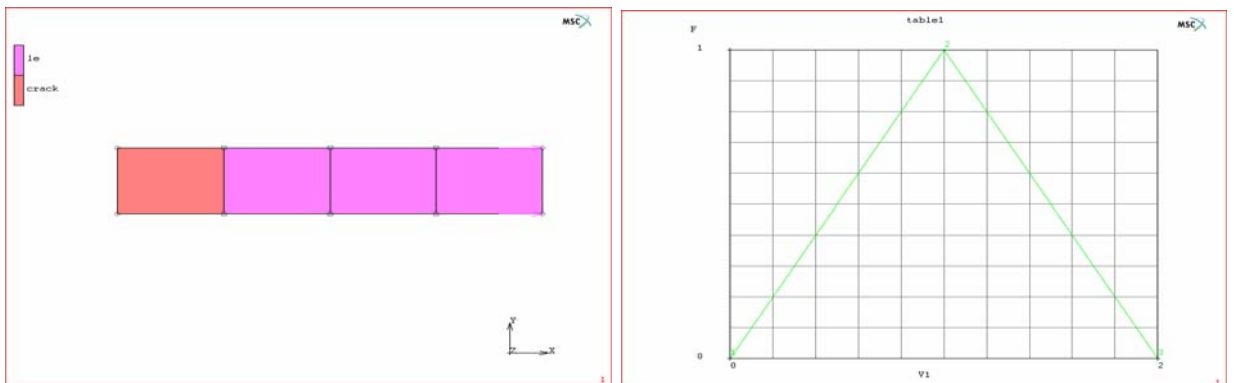


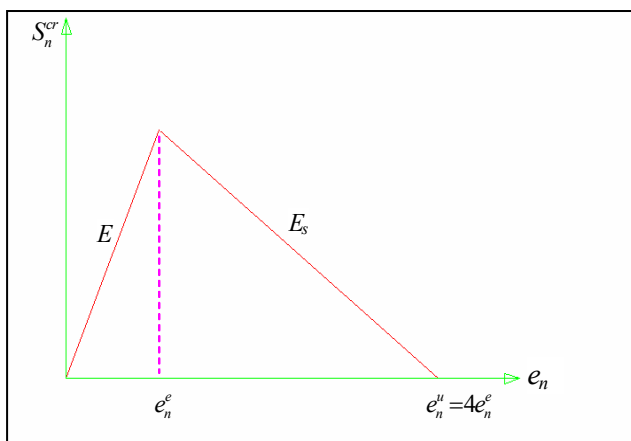
Figure 4.9 - Only one element softening  
(specimen 2)

Figure 4.10 - Applied load vs. time  
(specimen 2)

**3). Specimen 3** (tension specimen fixed at one end and pulled by node displacements at the other end). This specimen has the same model size (2 mm x 10 mm), the same material properties and the same boundary conditions as **Specimen 2**. As widely reported (de Borst

1986), local softening constitutive modelling of concrete could cause mesh-dependent results and even snap-back behaviour if the FE mesh is discretized differently for the same model. This non-objectivity regarding the mesh size could be eliminated if the non-local formulation, or the fracture energy based NLFM by adjusting the slope of the softening branch according to the magnitude of the fracture energy, is introduced into the constitutive model. This specimen is used to demonstrate that the phenomenon reported previously by de Borst (1986) can be modelled by the subprogram developed if the constitutive law is not adjusted according to the element size or other factors. The analysis of this specimen is designed to test the post-peak mesh-dependent problem existing in material fracture. The strain-softening constitutive relationship is shown in Figure 4.11. The ultimate strain  $\varepsilon_n^u$  is assumed to be four times the strain  $\varepsilon_n^e$  at the tensile strength. The shear retention factor  $\beta$  is arbitrarily assumed to be 0.2 as its value would not affect the results of this pure-tension specimen. The various subdivisions of the specimen are shown in Figures 4.13 to 4.17. In each case only the element on the left adjacent to the fixed boundary is allowed to crack.

The loading of node displacements is applied gradually up to the maximum value, as shown in Figure 4.12.



Young's modulus  $E = 20\,000$  MPa

Poisson's ratio  $\nu = 0$

Tensile strength  $f_t = 1.2$  MPa

Shear retention factor  $\beta = 0.2$  (arbitrary)

Applied node displacement = 0.0021 mm

Softening modulus  $E_s = -6\,666.67$  MPa

Figure 4.11 - Strain-softening diagram (specimen 3)

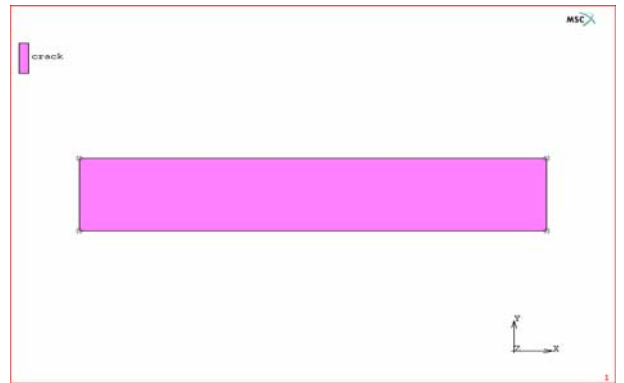
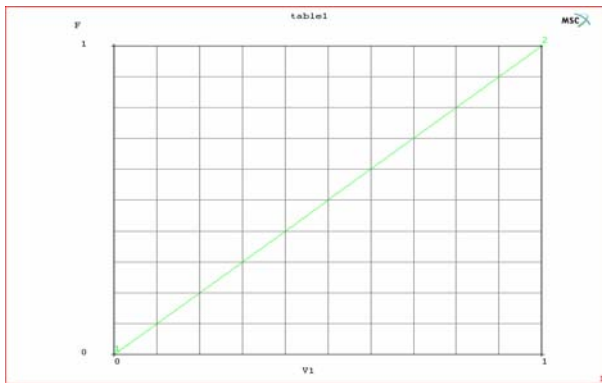


Figure 4.12 - Applied load vs. time (specimen 3) Figure 4.13 - Scenario 1: One element

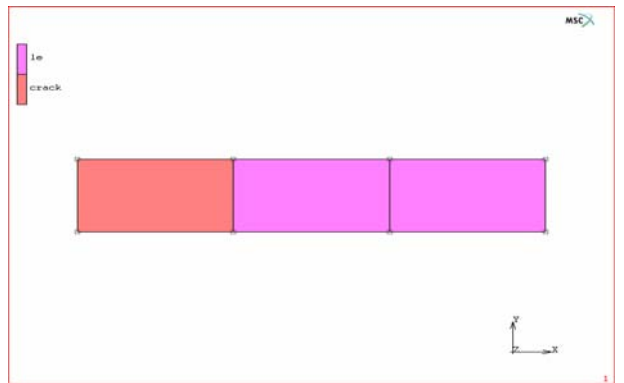
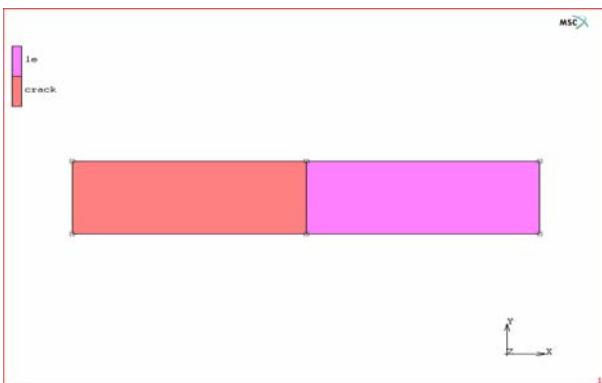


Figure 4.14 - Scenario 2: Two elements

Figure 4.15 - Scenario 3: Three elements

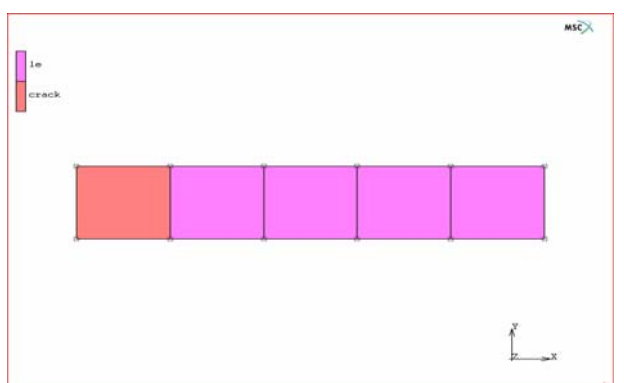
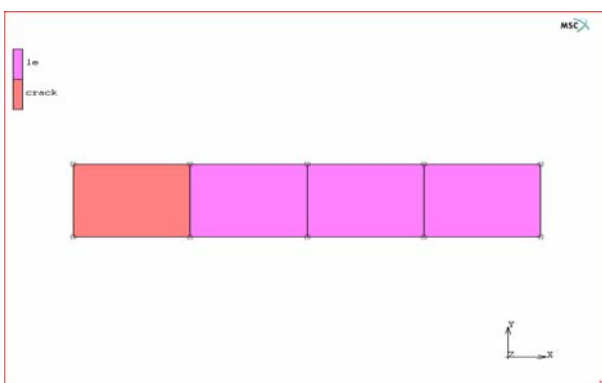


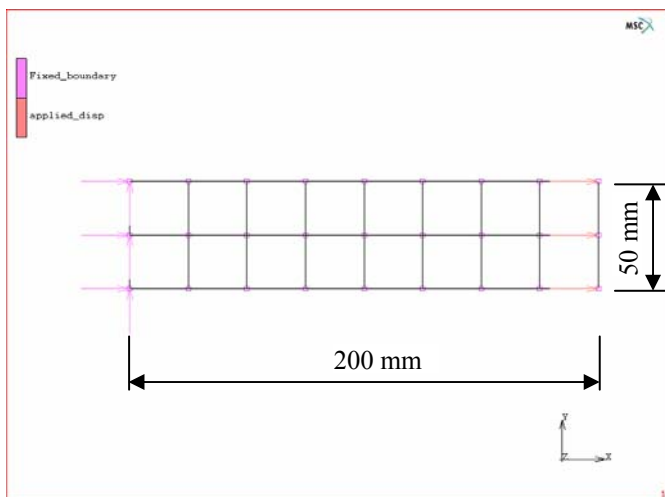
Figure 4.16 - Scenario 4: Four elements

Figure 4.17 - Scenario 5: Five elements

**4). Specimen 4** (A simple pure-tension specimen subjected to a constant stress field). A specimen (supported at one end, pulled at the other end – see Figure 4.18) of the unit thickness analyzed previously by Bhattacharjee & Leger (1993) is adopted to validate the

numerical implementation of the cracking model. This simple case is useful to confirm that the stress-strain response corresponds exactly to that of the material model. The FE model and the material properties are taken as the same as in the analysis of Bhattacharjee & Leger (1993) and are shown in Figure 4.18. For comparison purposes, a linear strain softening (see Figure 4.19) is selected and only the two elements at the fixed boundary are allowed to crack (see Figure 4.21). An arbitrary non-zero shear retention factor  $\beta$  is selected to stabilize the numerical solution since the  $\beta$  value will not influence the response of this mode I fracture analysis.

The loading of node displacements is applied gradually up to the maximum value, as shown in Figure 4.20.



Young's modulus  $E = 20\,000$  MPa  
 Poisson's ratio  $\nu = 0$   
 Tensile strength  $f_t = 2.0$  MPa  
 Fracture energy  $G_f = 0.04$  N/mm  
 Softening modulus  $E_s = -1\,333.33$  MPa  
 Thickness = 1.0 mm  
 Applied node displacement = 0.04 mm

Figure 4.18 - FE model – beam of 16 elements (specimen 4)

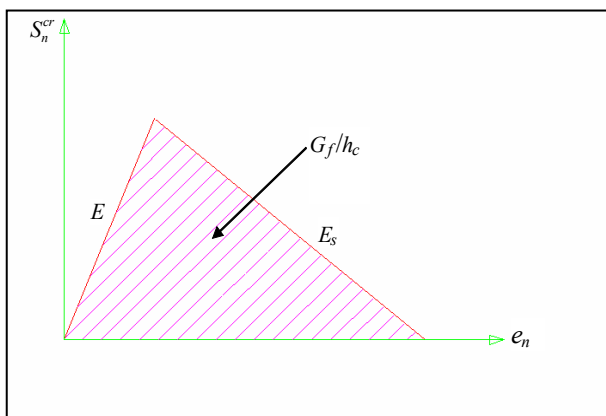


Figure 4.19 - Strain-softening diagram  
 (specimen 4)

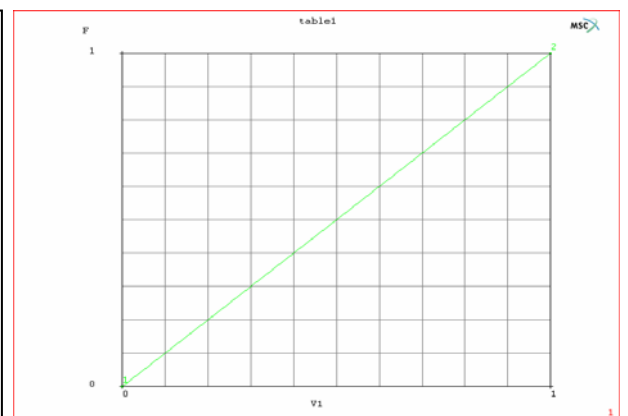


Figure 4.20 - Applied load vs. time  
 (specimen 4)

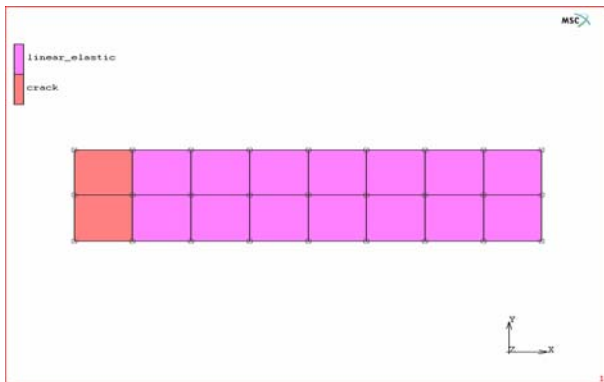


Figure 4.21 - Only the elements adjacent to rigid boundary softening (specimen 4)

#### 4.2.5 Discussion of results of the verification

The results from the four specimens analyzed are shown and discussed in this section.

**Specimen 1.** As seen from the following plots (Figures 4.22 to 4.24) of different softening moduli of 2 000, 20 000 and 50 000 MPa, the results from HYPELA are in very good agreement with those from the built-in crack model in MSC.Marc. This preliminary study shows that the subprogram HYPELA is capable of simulating cracking in this very simple one-element model.

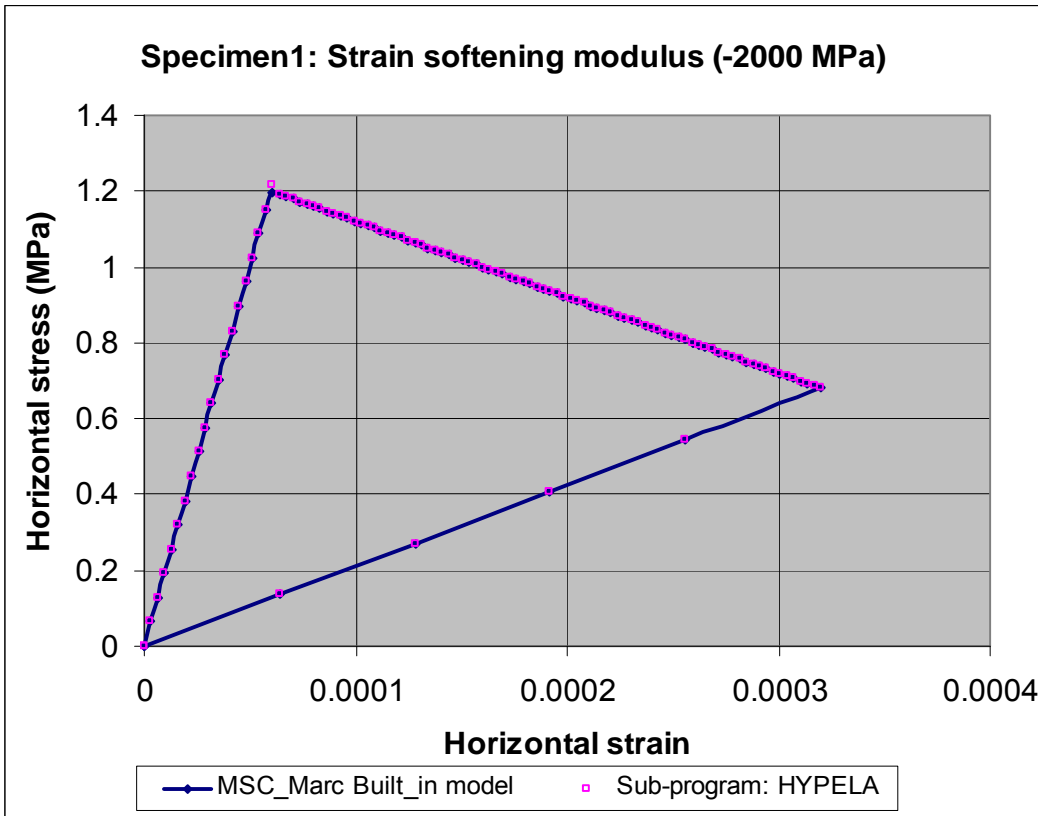


Figure 4.22 - Stress-strain plots for softening modulus  $E_s = -2\ 000$  MPa (specimen 1)

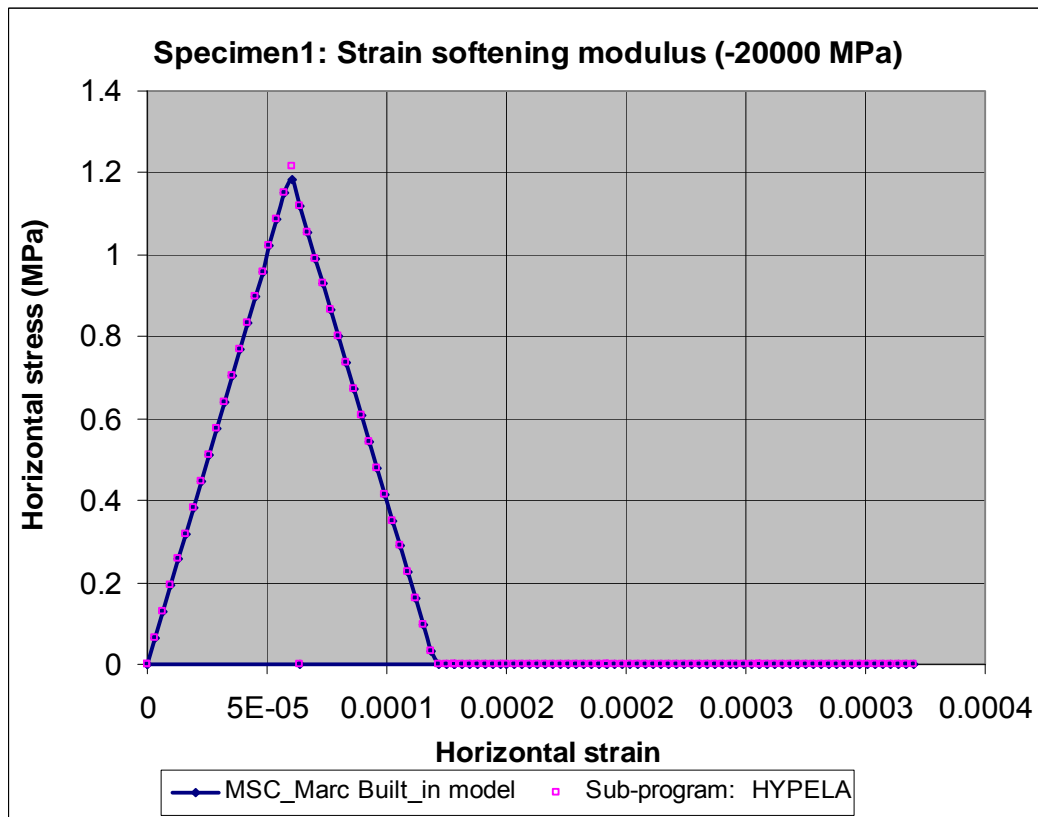


Figure 4.23 - Stress-strain plots for softening modulus  $E_s = -20\ 000$  MPa (specimen 1)

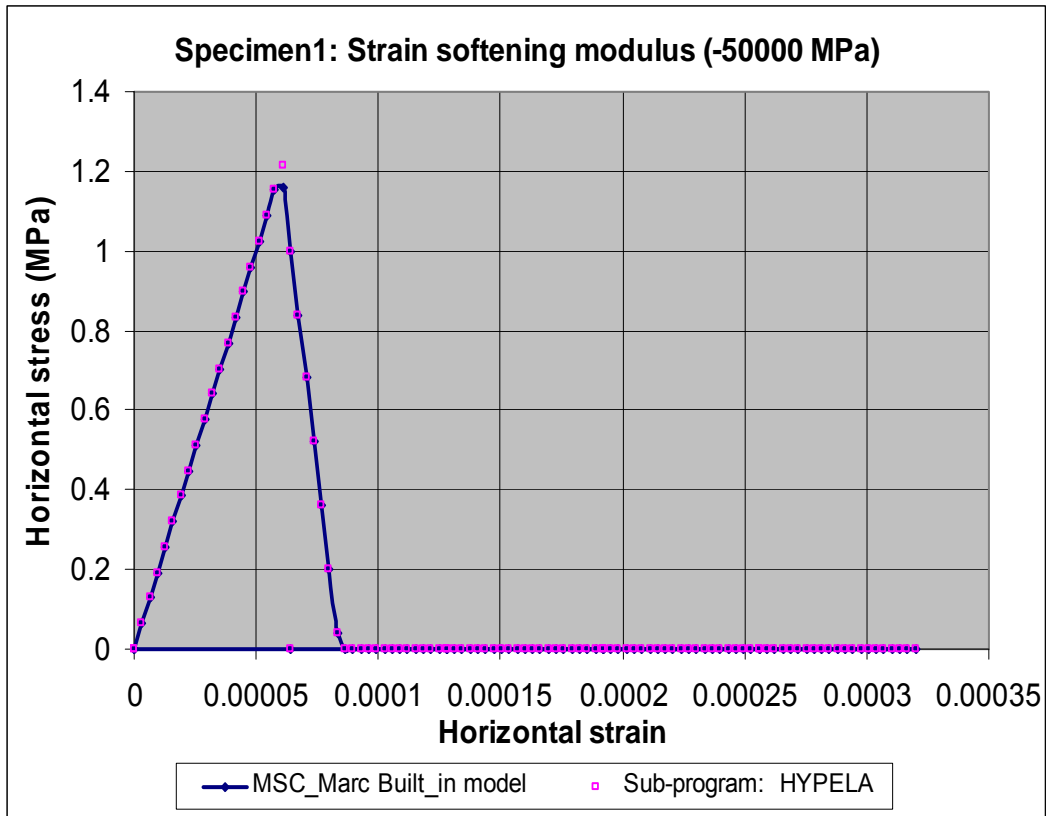


Figure 4.24 - Stress-strain plots for softening modulus  $E_s = -50\ 000$  MPa (specimen 1)

**Specimen 2.** The following stress-strain plots (Figures 4.25 to 4.27) of node 2 (shown in Figure 4.8) for different softening moduli of 2 000, 5 000 and 20 000 MPa show that the results from HYPELA are in excellent agreement with those from the built-in crack model in MSC.Marc. This again shows that the subprogram HYPELA is capable of simulating cracking in this four-element model.

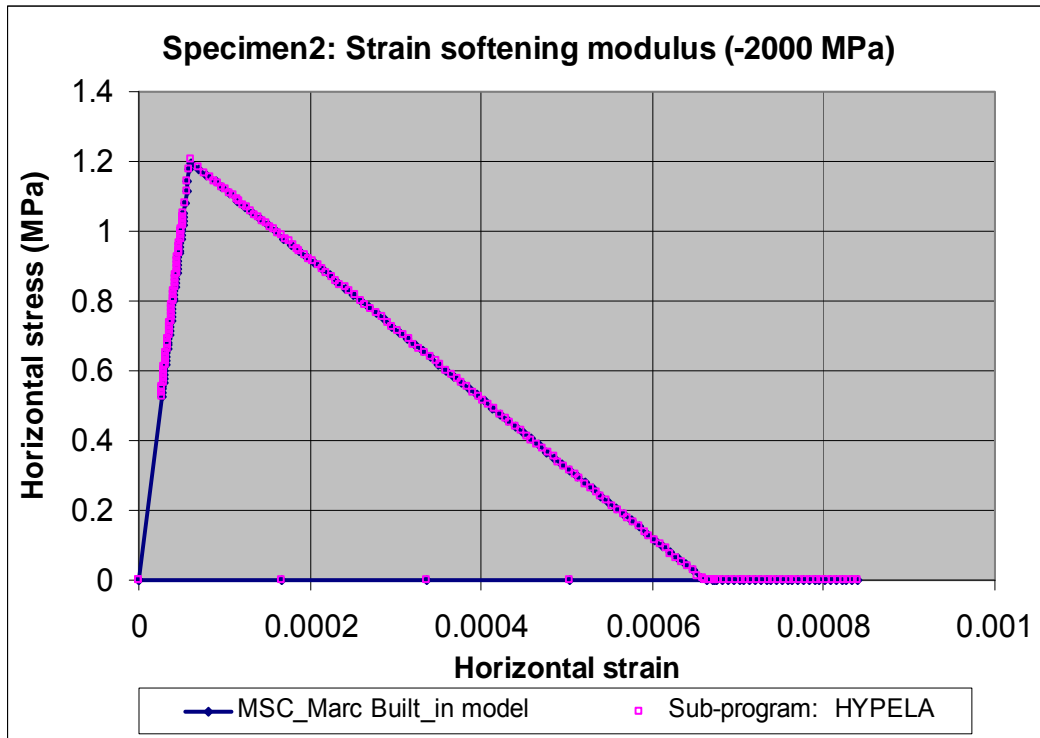


Figure 4.25 - Stress-strain plots (softening modulus  $E_s = -2\ 000$  MPa) (specimen 2)

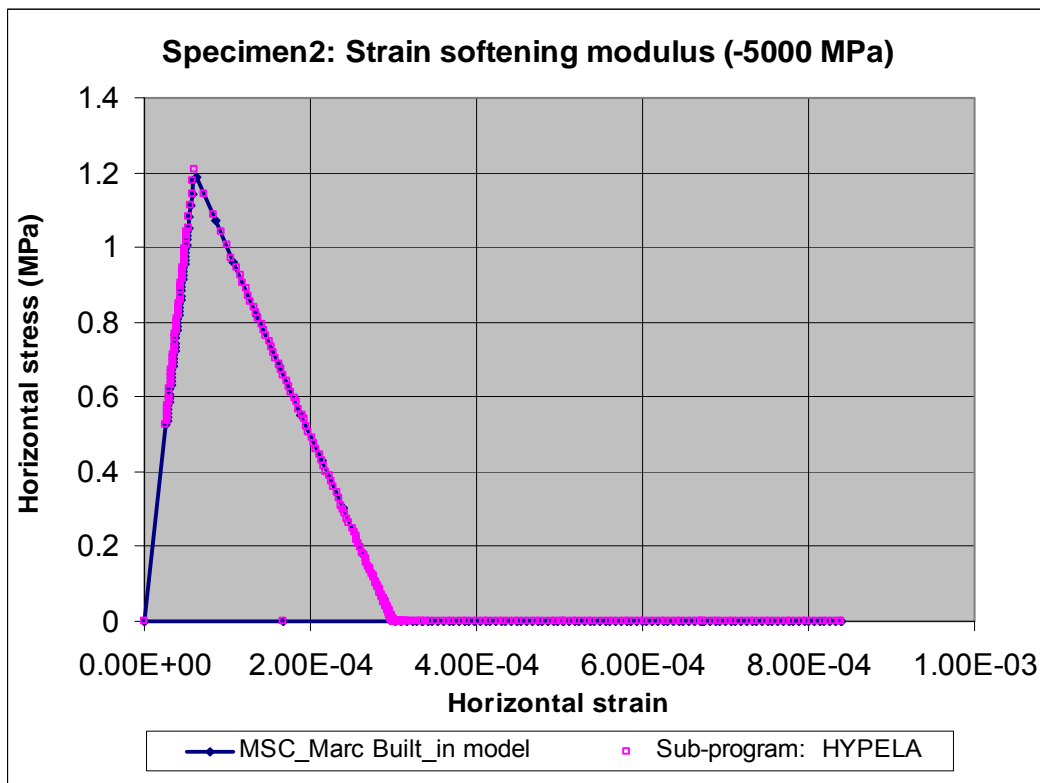


Figure 4.26 - Stress-strain plots (softening modulus  $E_s = -5\ 000$  MPa) (specimen 2)



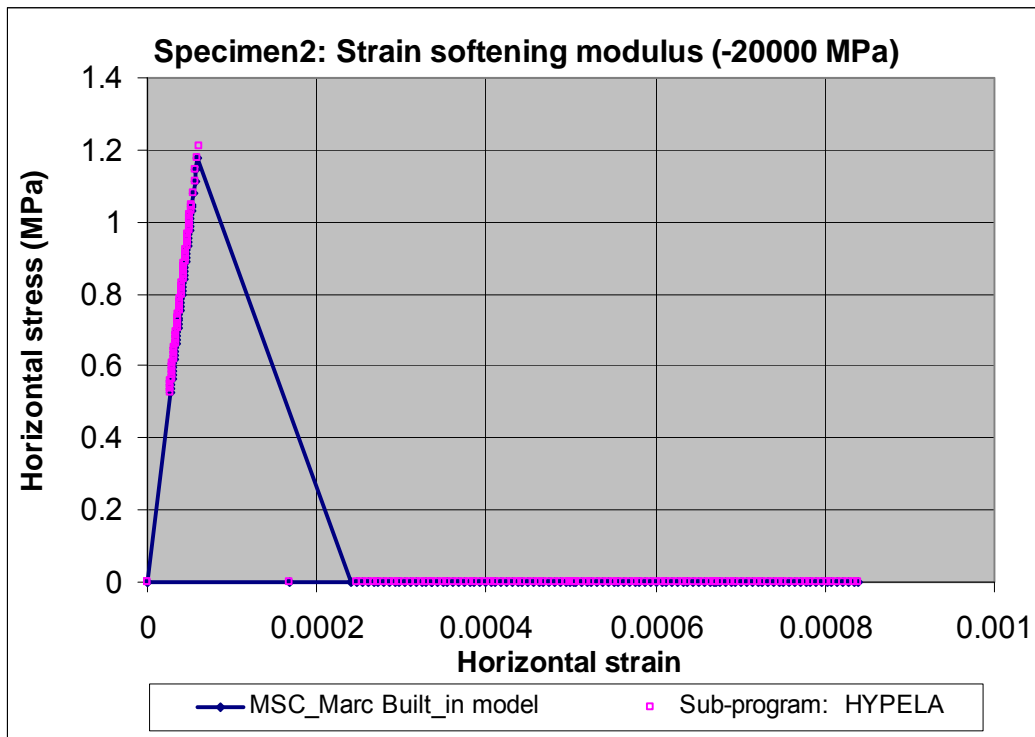


Figure 4.27 - Stress-strain plots (softening modulus  $E_s = -20\ 000$  MPa) (specimen 2)

**Specimen 3.** The model shows that when one element is cracking, the other elements are unloading correctly. Figure 4.28 shows that after the assumed tensile strength  $f_t = 1.2$  MPa has been reached, as the FE model is meshed with an increasing number of elements, the averaged horizontal strain of the model decreases until a value of zero averaged strain increment is obtained when the model is meshed with four elements. This four-element model of zero averaged strain increment corresponds to the linear strain-softening modulus chosen, which has an ultimate strain  $\varepsilon''$  four times the strain at the tensile strength (refer to Figure 4.11). If the number of elements in the model is greater than four, the snap-back phenomenon appears. In other words, as the model is discretized with more and more elements (up to five elements), the averaged strain of the model is gradually decreased and even snapped back as indicated by de Borst (1986).

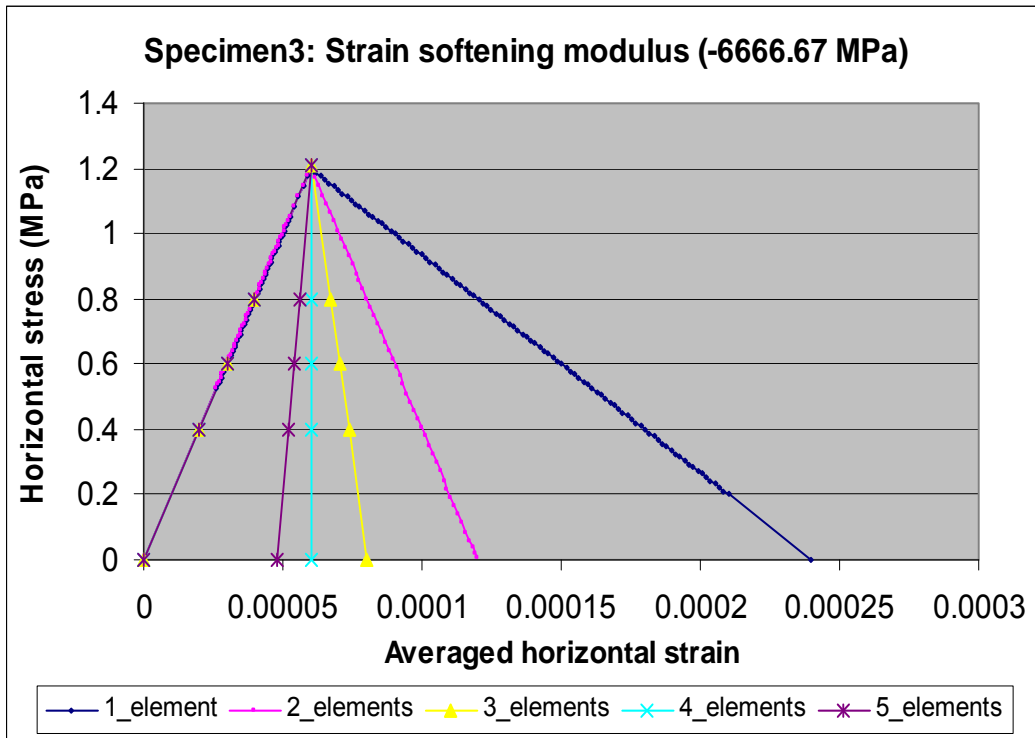


Figure 4.28 - Averaged strain for different numbers of elements in the model (specimen 3)

**Specimen 4.** This simple, pure-tension beam was designed for the verification of mode I (opening) concrete fracture, which is widely regarded to be the dominant mode for most concrete structures. The calculated force-displacement response is shown in Figure 4.29 demonstrating very close agreement with the results of Bhattacharjee & Leger (1993) and further validating the numerical implementation of HYPELA for the crack models adopted.

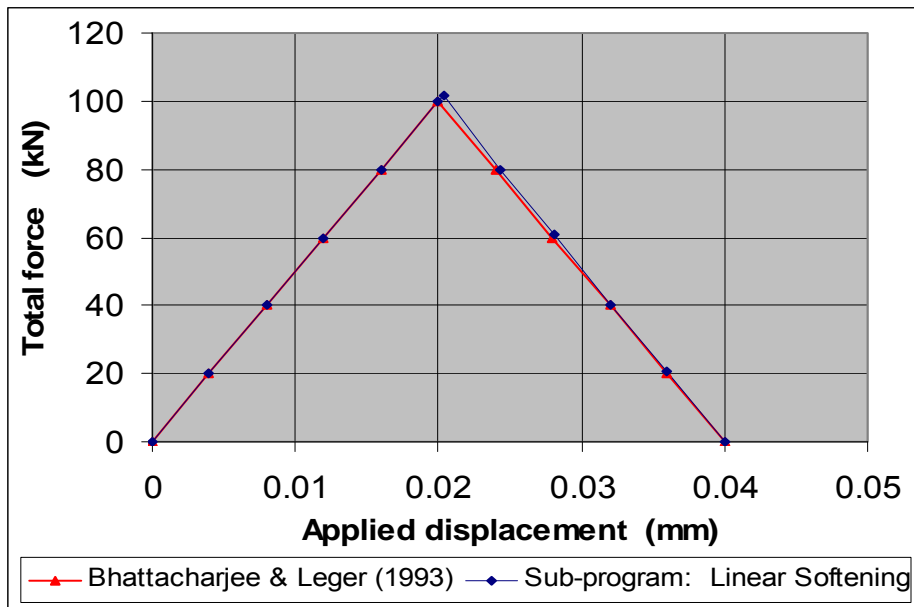


Figure 4.29 - Force-displacement response (specimen 4)

#### 4.3 Verification study with DIANA

The commercial general-purpose FE program DIANA (DIANA 1998) is a well-known code for non-linear crack analysis. Three cracking-verification cases in DIANA are selected to further benchmark the subprogram HYPELA.

Second-order plane strain elements with four integration points are used in this verification study (Figure 4.30).

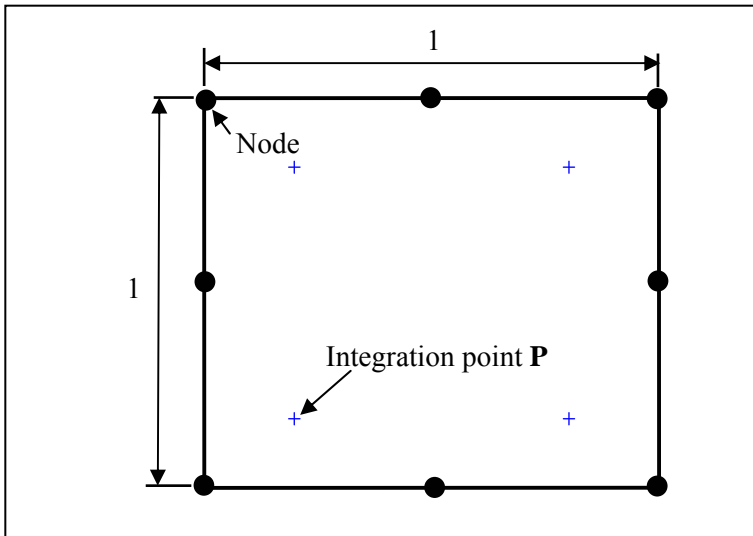


Figure 4.30 - Second-order plane strain element

The specimens are fixed on one side and pulled at the other side by a horizontal deformation  $\delta x = 1.0E-4$ , which is multiplied by a factor of  $f$ , as shown in Figure 4.31.

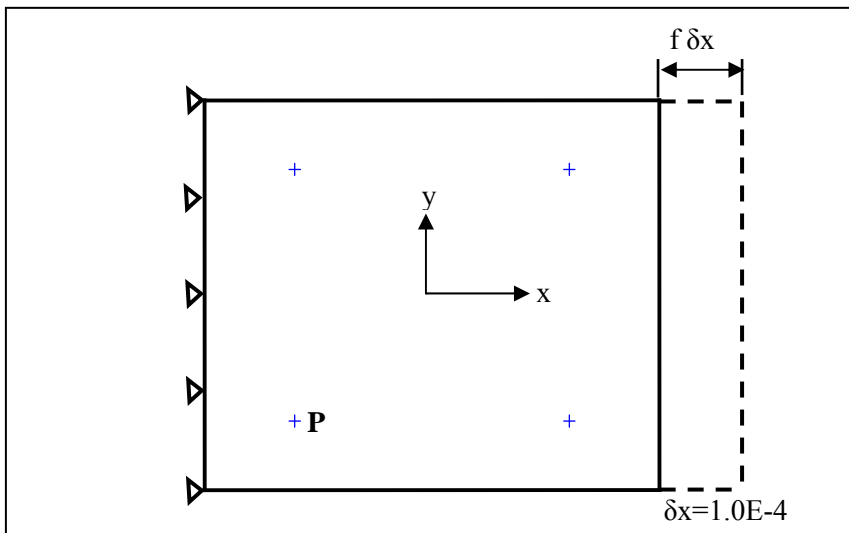


Figure 4.31 - Boundary and loading

The purpose of these case verifications is to check the consistency of the crack status, crack strain and total stress for the integration point  $P$  after each loading step.

#### 4.3.1 Cracking with linear tensile softening – plane strain (called PET1CR in DIANA)

Smearred cracking with linear tension softening and full shear retention are applied. The loading is deformation, applied in six steps up to  $f = 41,1$ . The results shown in Figure 4.32 indicate that the proposed smearred crack model coded in the subprogram HYPELA produces the same results as those from DIANA.

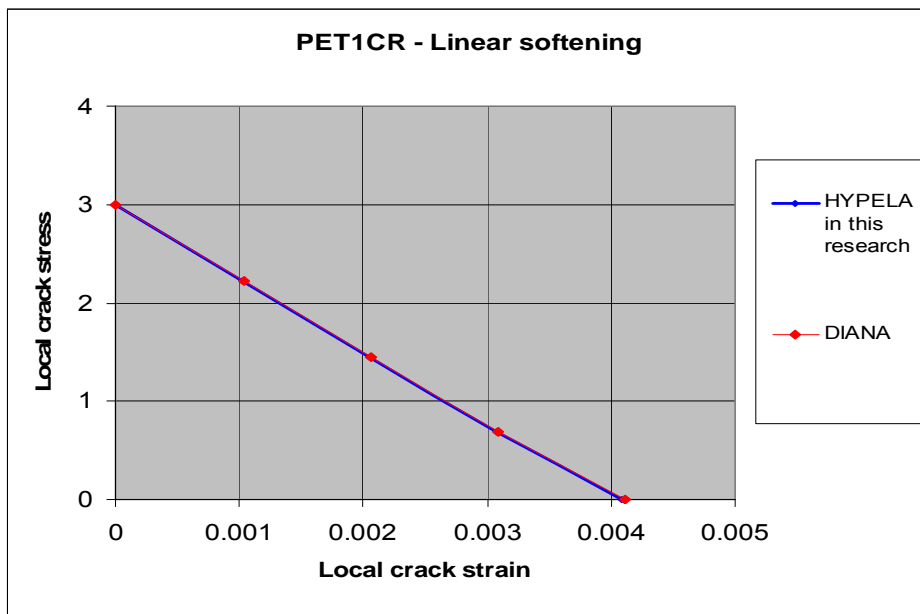


Figure 4.32 - Crack stress and crack strain response (PET1CR)

#### 4.3.2 Cracking with bilinear tensile softening – plane strain (PET2CR)

Smearred cracking with bilinear tension softening and full shear retention are applied. The loading is deformation, applied in six steps up to  $f = 41,1$ . The results in Figure 4.33 show that the HYPELA subprogram produces the same results as those from DIANA.

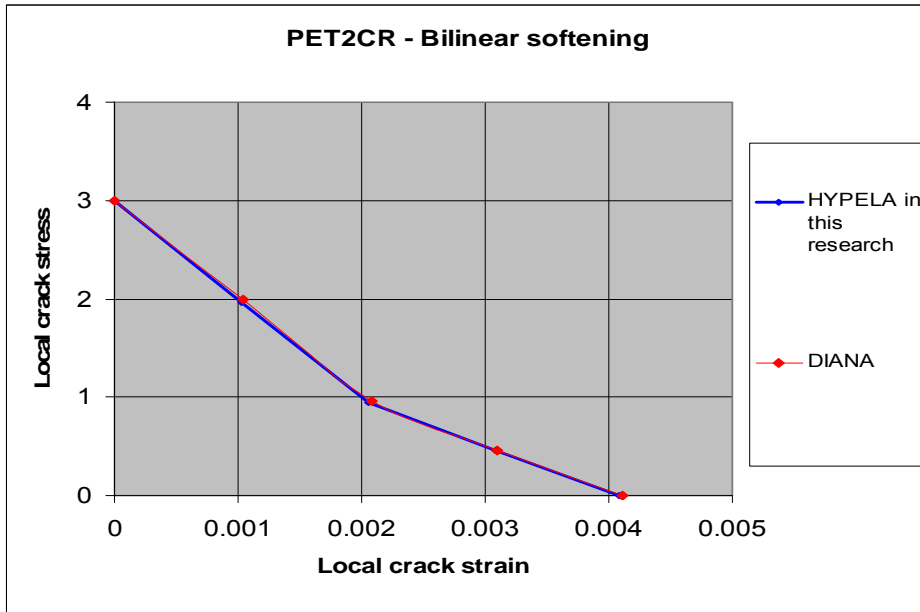


Figure 4.33 - Crack stress and crack strain response (PET2CR)

#### 4.3.3 Cracking with alternating loading – plane strain (PECLOP)

Smearred cracking with linear tension softening and full shear retention are applied. The loading is deformation, applied in ten alternating steps, as shown in Figure 4.34. The crack closes and reopens due to the alternating loading. The results shown in Figure 4.35 indicate that the HYPELA subprogram developed in this chapter can correctly model crack closing and reopening.

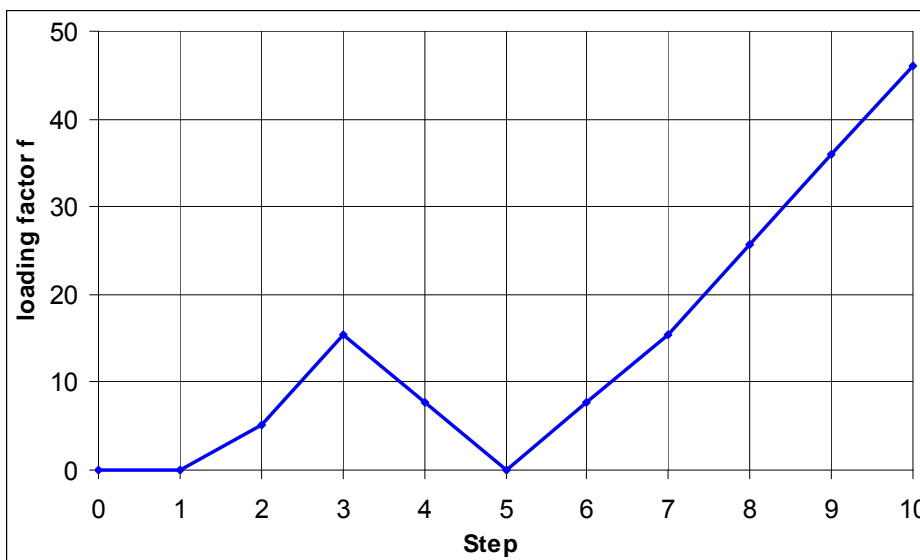


Figure 4.34 - Loading factor f at steps (PECLOP)

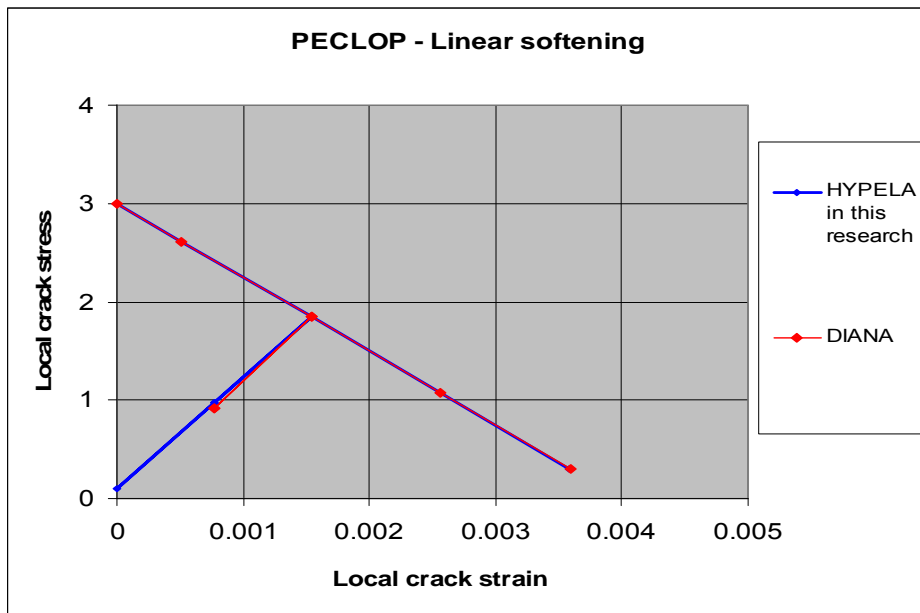


Figure 4.35 - Crack stress and crack strain response (PECLOP)

#### 4.4 Concluding remarks

Incorporated into the commercial general-purpose FE program MSC.Marc, a subprogram called HYPELA has been coded to model the non-linear cracking process in concrete, using the smeared crack models developed previously for constitutive stiffness adjustment. For the plane stress elements, the subprogram was thoroughly benchmarked and verified in the four chosen FE models (mode I), either specially designed for this verification purpose or previously numerically tested. The HYPELA subprogram was further verified using plane strain elements, which showed good correlation with DIANA.

Based on this first-stage benchmark exercise, which was intended to test the implementation procedure on elementary, simple specimens, the subprogram developed for this research can be used with confidence for further validation on more complicated concrete cracking structures, including concrete gravity dams, and eventually for the constitutive cracking analysis of a real concrete dam.

The crack model outlined in Chapter III will also be used to benchmark and validate the crack models and the numerical implementation procedure in the analysis of mode I and mixed-mode concrete beams in Chapter V and in the analysis of concrete gravity dams in Chapter VI. The benchmark studies in Chapters V and VI are more detailed and

complicated for the purpose of thoroughly testing the versatility of the coded subprogram. Eventually, the crack models and numerical techniques that have been developed will be applied in the cracking analysis of a real gravity dam in South Africa and in the evaluation of the safety of the dam.